Mechanical Alloying of Dispersion-Hardened Ni_3Al-B from Elemental Powder Mixtures

E.H. Yoon, J.K. Hong, and S.K. Hwang

Mechanical alloying and hot extrusion were studied as a means to dispersion harden an intermetallic compound based on Ni_3Al-B from elemental powder mixture. The oxide used for the dispersoids was partially stabilized zirconia. During mechanical alloying the microstructure evolved according to the characteristic stages found in other mechanical alloying systems. Completion of the alloying reaction required 16 h, beyond which loss of the crystalline property set in. Experimental observation of the grain refinement during mechanical alloying agreed with a prediction based on an existing model. Compared to V-cone mixing, the mechanical alloying produced a homogeneous distribution of fine dispersoids. The refined grain structure and dispersoids resulted in a high tensile yield strength over a wide range of temperatures.

Keywords
dispersion-hardened, mechanical alloying, mechanical properties, Ni_3Al-B-ZrO_2

1. Introduction

INTERMETALLIC COMPOUNDS based on Ni_3Al have attractive high-temperature mechanical properties, such as high specific strength and good oxidation and creep resistance (Ref 1, 2). By adding boron to the composition, Aoki and Izumi (Ref 3, 4) enhanced the tensile ductility remarkably. Recently, various processing techniques, including powder metallurgical methods, have been under evaluation in attempts to synthesize the alloy for successful practical application (Ref 5-9). We reported that a direct extrusion method starting from a mixture of elemental powders produced a high strength and tensile ductility in this alloy (Ref 10). To enhance the tensile strength and the creep resistance of the alloy further, dispersion hardening the compound with ZrO_2 was also tried (Ref 11). However, the zirconia powder particles coagulated during mixing and caused an inhomogeneous distribution after the powder extrusion (Ref 12). The present work was undertaken to solve this problem. This paper focuses on the effect of mechanical alloying technique (Ref 13-17) in achieving a dispersion hardening in Ni_3Al-B alloy processed from elemental powder mixtures. Two objectives were set for the present research: to confirm the feasibility of homogeneous alloying and to enhance the yield strength by controlling phase constitution and microstructure.

2. Experimental Procedure

The chemical composition of the experimental alloy consisted of Ni_3Al with a slightly higher content of nickel than stoichiometry, boron, and partially stabilized zirconia (PSZ) with 3 mol% Y_2O_3. Nickel, aluminum, and all the alloying additives were mixed from elemental powders. Table 1 shows the chemical composition of the alloy and the characteristics of the powders used in this study.

E.H. Yoon, Dae-Chang Industries Co., Inc., Anyang, Korea; **J.K. Hong,** Fine Semitech Co. Ltd., R&D Center, Suwon, Korea; and **S.K. Hwang,** Inha University, Dept. of Metallurgical Engineering, Inchon, Korea.

Table 1 Nominal compositions of the experimental alloys

	Composition, wt% (a)			
Alloy	Ni	Al	B	PSZ(b)
Ni_3Al	87.4	12.60	...	...
Ni_3Al-B	87.3	12.60	0.10	...
Ni_3Al-B-PSZ	85.0	12.35	0.15	2.5

(a) Mean particle size, µm: Ni, 4.5; Al, 5; B, 1; PSZ, 0.3. (b) Partially stabilized zirconia, ZrO_2 + 3 mol% Y_2O_3

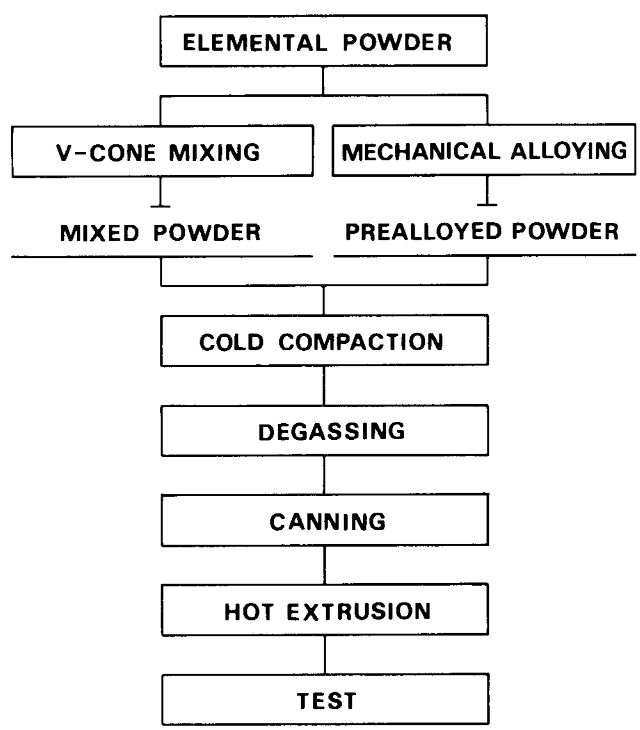

Fig. 1 Flow chart of the experimental procedure

For mechanical alloying, an attritor with vertical rotating shaft was used. The inner volume of the milling jar and the diameter of the ball were 0.75 L and 4.8 mm, respectively. The weight ratio of the elemental powder mixture to balls was 1:35. The mechanical milling was done in an argon atmosphere at a rotating speed of 300 rpm, and the milling time was varied

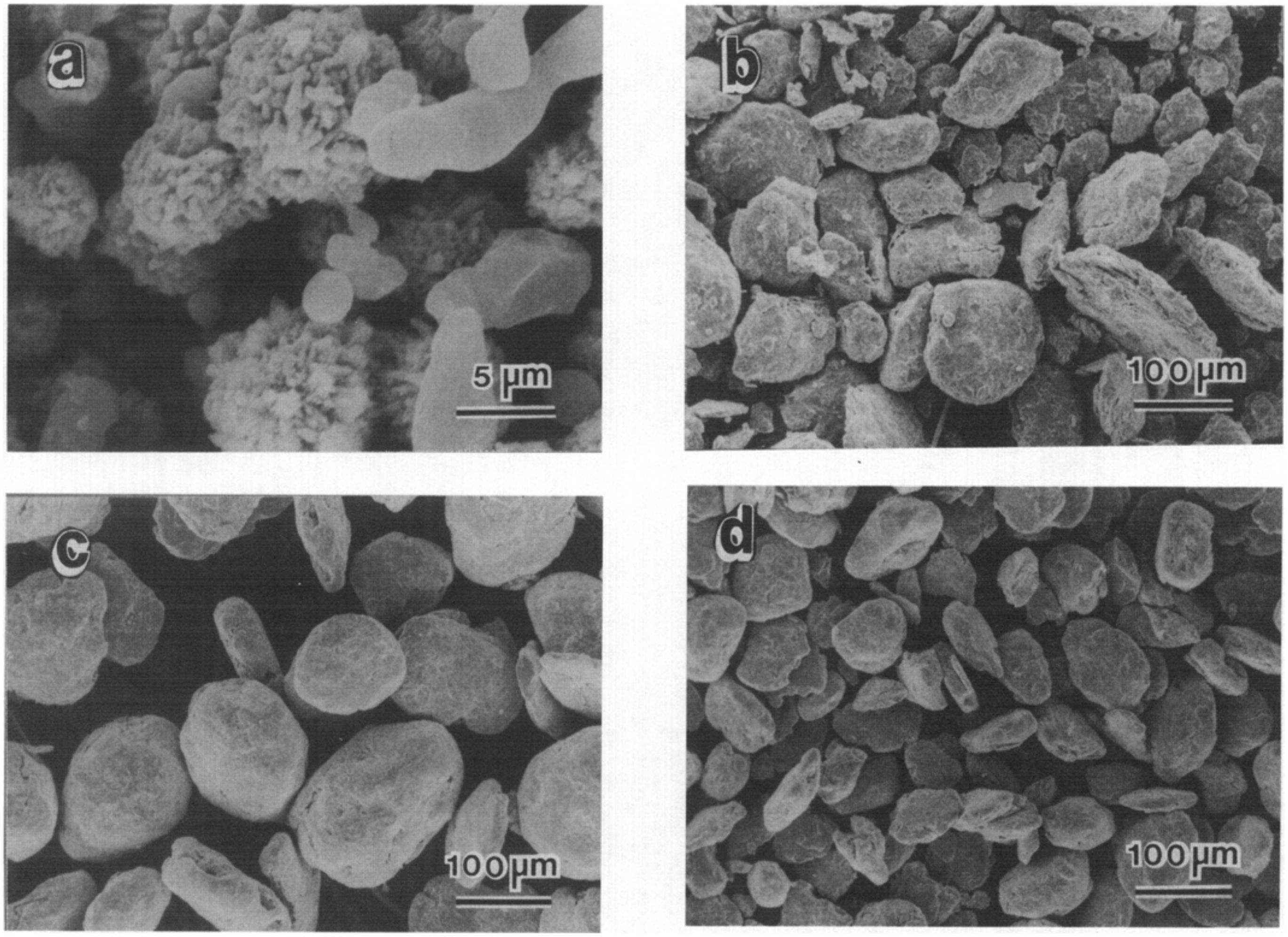

Fig. 2 Scanning electron micrographs of Ni_3Al that was mechanically alloyed from elemental powders for various amounts of milling time. (a) 0 min. (b) 40 min. (c) 6 h. (d) 16 h

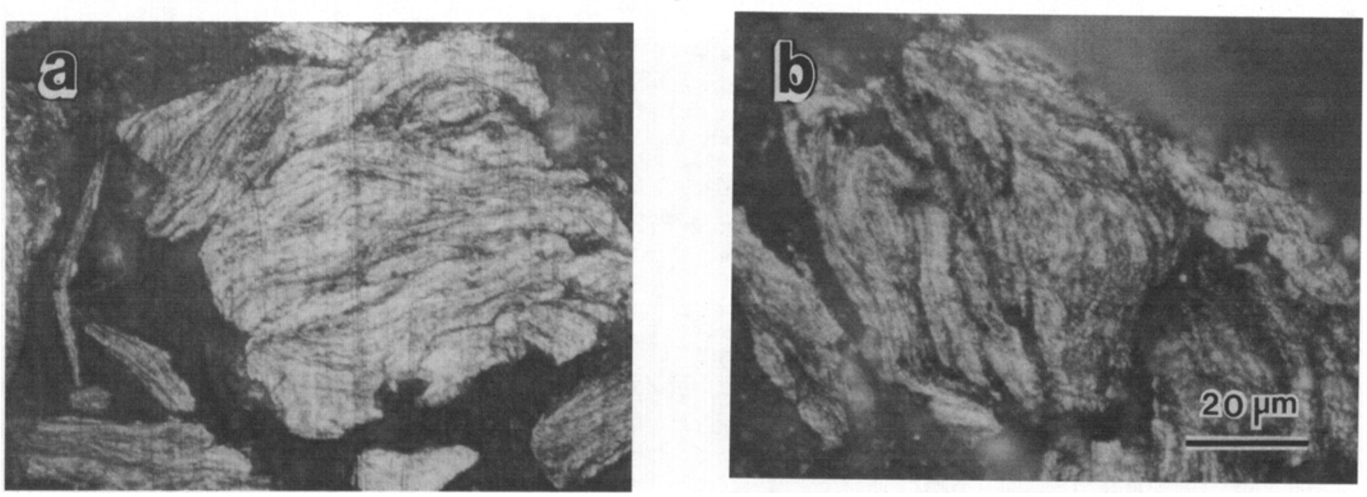

Fig. 3 Optical micrographs of Ni_3Al that was mechanically alloyed from elemental powders milled for (a) 2 h or (b) 4 h

from 10 min to 24 h. Another mixing method, V-cone mixing, consisted of 40 min of tumbling at 50 rpm in a 2 L container.

Hot extrusion was used to consolidate the elemental mixtures made by either the attritor or the V-cone mixer. The powder mixtures, canned in a mild steel cylinder, underwent compaction at 300 MPa and degassing treatment at 450 °C under 0.1 Pa. Then the cans were extruded at 1000 °C with a reduction ratio of 18:1. Figure 1 illustrates the flow of the experimental procedure.

Using the x-ray diffraction technique, we analyzed the lattice parameter variation using Cohen's method (Ref 18). The exothermic heat of reactive sintering with differential thermal analysis (DTA) was also measured. Tensile properties of the experimental alloys were measured at various temperatures, up to 800 °C, with a strain rate of 2×10^{-3} s^{-1}. Tensile specimens had a gage length and gage diameter of 16 mm and 4 mm, respectively.

3. Results

3.1 *Mechanical Alloying*

The morphology of the powder particles changed with milling time, as shown in Fig. 2. Elemental powder particles with the mean size of 4.75 μm became thin platelets at 40 min. During the initial period of milling, a large compressive stress at the interface of the balls and powder caused a rapid coarsening of powders. A lamellar structure appeared subsequently.

The lamellar structure became most apparent between 2 and 4 h, as shown in Fig. 3(a). Successive collisions and weldings during this period resulted in platelets of 100 μm in average thickness. The interlamellar spacing decreased and the orientation of the lamellae became randomized with time, as shown in Fig. 3(b). Due to the random collisions, the lamellar structure changed with time from a regular layer to a spherical shape.

With increased milling time the particles showed a mixed morphology of platelets and spheres of about 120 μm in size. Figures 2(c) and (d) show the particle shapes at 6 and 16 h, respectively. The particle size did not change up to 10 h, but after that it decreased due to particle fracture. At 16 h the particles showed a uniform spherical size of about 60 μm, as shown in Fig. 2(d). This stage was followed by a steady state up to 24 h, during which time the particle size remained constant and the fine lamellar structure became obliterated. During the steady-state period, the collision-welding process of particles appeared to balance the fracturing process.

Microhardness of individual alloyed powder particles varied with milling time, as shown in Fig. 4. The hardness increased from 250 to 700 H_V as the milling time reached 10 h, after which it remained constant. This is presumably due to the onset of a dynamic recovery promoted by the plastic energy accumulated during milling.

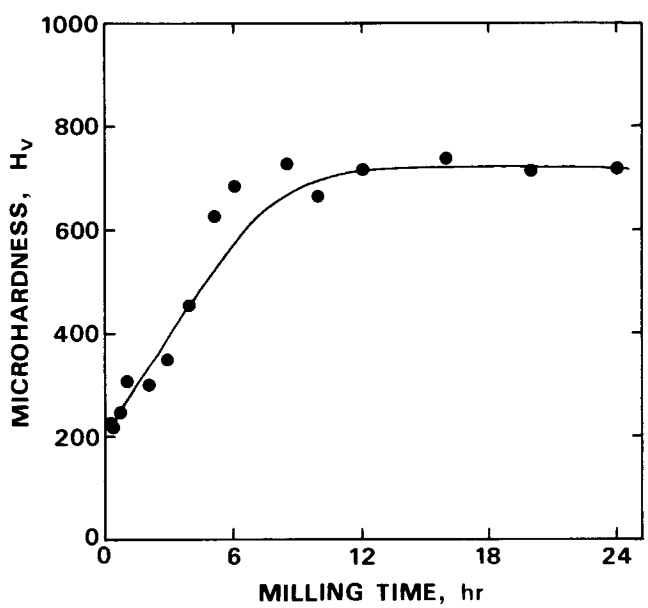

Fig. 4 Microhardness as a function of milling time of Ni_3Al that was mechanically alloyed from elemental powders

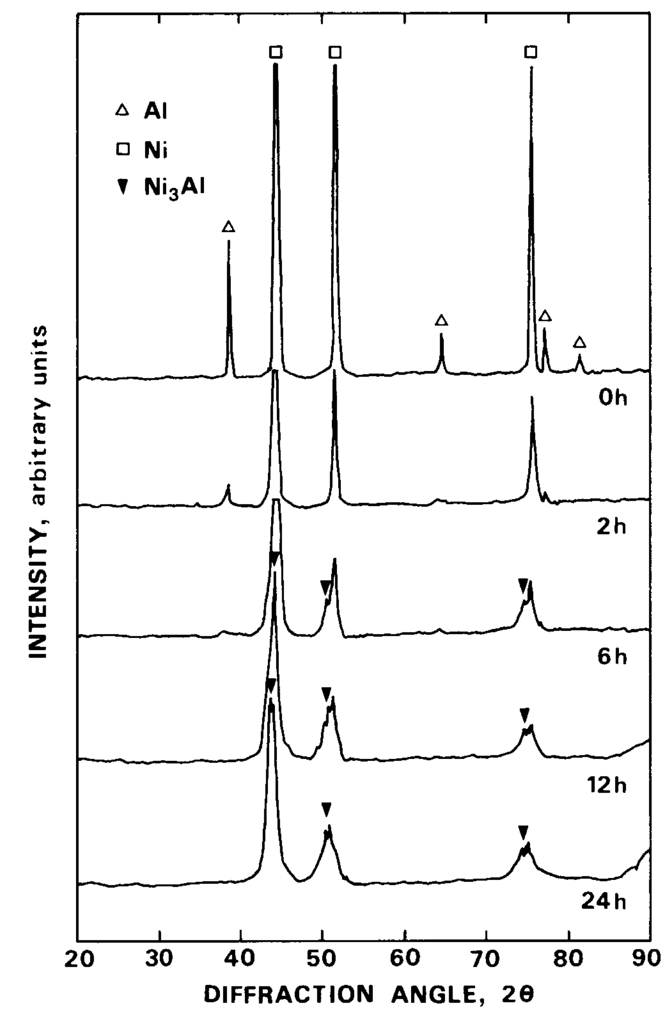

Fig. 5 X-ray diffraction patterns of Ni_3Al that was mechanically alloyed from elemental powders milled for various amounts of time

Figure 5 shows x-ray diffraction spectra of samples obtained after various milling times. As the milling time increased, the peak intensity generally decreased, whereas the peak width increased due to plastic deformation. The ratio I_{Al}/I_{Ni}, where I is intensity, decreased with milling time because aluminum dissolved in nickel. A Ni_3Al peak appeared first in the specimen milled for 6 h. Completion of the alloying reaction required 16 h, beyond which the alloy started to lose crystallinity and became increasingly amorphous.

The lattice parameters of the crystalline phases also changed with milling time, as shown in Fig. 6, but the trend varied with the element: The lattice parameter of nickel increased with time while that of aluminum showed a reverse trend. The lattice parameter of Ni_3Al increased with milling time, reaching 3.570 Å at 10 h. A further increase of the lattice parameter during prolonged milling, 3.585 Å at 24 h, coincided with the appearance of the amorphous state.

The DTA results presented in Fig. 7 confirms the progressive alloying of Ni_3Al during mechanical milling, as found from the microstructure and the lattice parameter. The amount of heat evolving from the exothermic reaction varied with milling time, reaching a maximum at 1 h and gradually decreasing with further milling. From 16 h on, no peak was discernible in the DTA curve. The reduced heat evolution indicates that the amount of liquid phase required for Ni_3Al formation decreased.

Figure 7 also shows that the temperature corresponding to the main exothermic reaction decreased with milling time. This is because the driving force for the alloying reaction increases with time. Microstructural evolution such as the lamellar structure refinement or defects introduced during milling promote solid-state diffusion between elemental powder particles. Consequently, the exothermic reaction among powder particles in the mixture occurred at a temperature lower than the lowest eutectic temperature in the Ni-Al system, 640 °C.

Table 2 Microhardness of hot extruded Ni_3Al-B system alloys

Alloy	Process(a)	Grain size, μm	H_v, kg/mm^2
Ni_3Al-B	VM + HE	7	422
Ni_3Al-B-PSZ	VM + HE	6	474
	MA + HE	2	662

(a) VM, V-cone mixing; MA, mechanical alloying; HE, hot extrusion

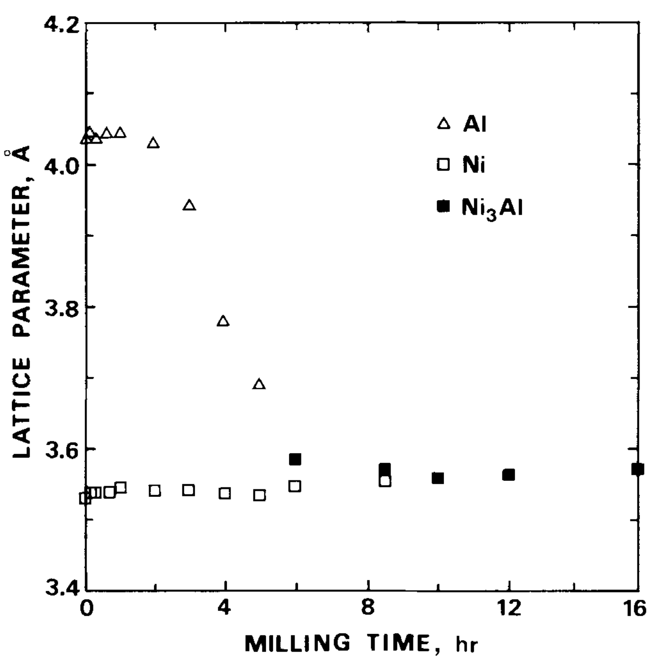

Fig. 6 Lattice parameters as a function of milling time for nickel, aluminum, and Ni_3Al powders

3.2 *Hot Extrusion*

Hot extrusion of either V-cone-mixed or mechanically alloyed powder resulted in a high microhardness, the effect being particularly significant in the latter. The effect of PSZ addition was also conspicuous in mechanically alloyed powder. While the microhardness increment due to PSZ addition was 10% for V-cone-mixed alloy, it was 40% for the mechanically milled alloy. Table 2 shows the grain size and the microhardness of experimental alloys prepared by various processing methods. There are several reasons for the pronounced hardening in the mechanically alloyed and hot extruded PSZ-containing alloy: grain refinement (down to 2 μm), uniform distribution of the dispersoids, and work hardening.

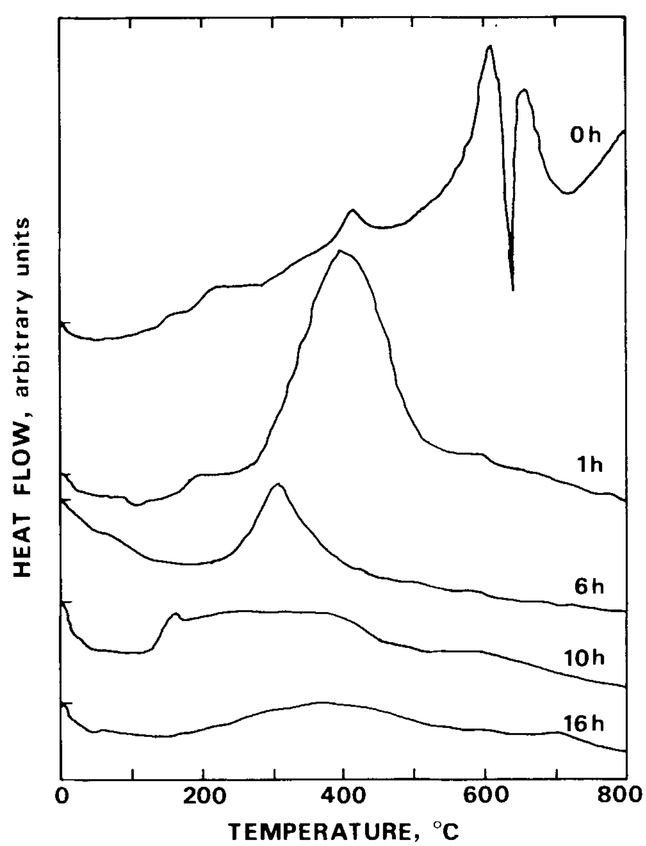

Fig. 7 Differential thermal analysis scan of Ni_3Al that was mechanically alloyed from elemental powders milled for various amounts of time

Microstructural evidence for the heterogeneous distribution of PSZ in the V-cone-mixed and hot extruded alloy is shown in Fig. 8. PSZ powder of 0.3 μm in average size before mixing grew to 60 to 70 μm by agglomeration during mixing. This phenomenon was not observed in the mechanically alloyed material.

The microstructural characteristics shown in Table 2 and Fig. 8 explain the difference in the tensile properties of experimental alloys, as listed in Table 3. V-cone mixing treatment rendered good tensile ductility in PSZ-free alloy. However, for the PSZ-containing alloy, V-cone mixing resulted in a low yield strength due to premature cracking. In contrast, the mechanical alloying treatment of the same alloy enhanced the yield strength to 1640 MPa, which is greater than what Benn et al. (Ref 14) reported for $Ni_3Al\text{-}Al_2O_3$ alloy. As mentioned above, the coarse PSZ particles that agglomerated during mixing remained after hot extrusion and which acted as vulnerable sites for crack initiation and propagation.

The characteristics of the tensile properties at room temperature were reproduced at elevated temperature. Figure 9 shows the yield strength of variously processed alloys as a function of temperature. Below 800 °C, V-cone mixing was a favorable treatment for the PSZ-free alloy, whereas it was ineffective for the PSZ-containing alloy. Mechanical alloying, however, produced a remarkably high yield strength in the PSZ-containing alloy at high temperature, up to 400 °C. It is noted in Fig. 9 that the anomalous yielding feature disappeared in this alloy. Above 400 °C, the yield strength decreased rapidly with temperature like other mechanically alloyed Ni_3Al, as reported by Benn and Hiroki (Ref 14, 19). This is presumably due to the fine grain size and dispersion hardening.

The beneficial effect of mechanical alloying on the yield strength appeared as detrimental to the tensile ductility. Figure 10 shows the variation of the tensile elongation with temperature. While V-cone mixing produced as high as a 13% tensile elongation in the extruded condition, mechanical alloying reduced the tensile ductility. This is in part due to oxidation dur-

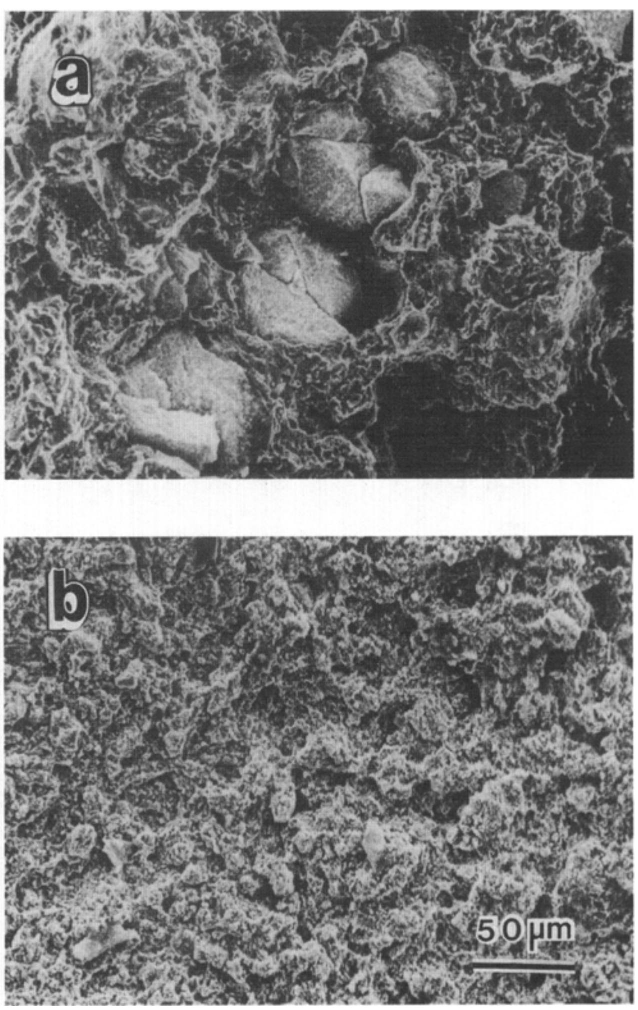

Fig. 8 Scanning electron fractographs of tensile-tested Ni_3Al-B-PSZ alloys made from elemental powders. (a) V-cone mixed and hot extruded. (b) Mechanically alloyed and hot extruded

Table 3 Room-temperature tensile properties of hot-extruded and dispersion-strengthened Ni_3Al-B alloys

Alloy	Process(a)	Yield strength, MPa	Ultimate tensile strength, MPa	Elongation, %
Ni_3Al-B	VM + HE	840	1393	41
Ni_3Al-B-PSZ	VM + HE	796	987	13
	MA + HE	1636	1655	1

(a) VM, V-cone mixing; MA, mechanical alloying; HE, hot extrusion

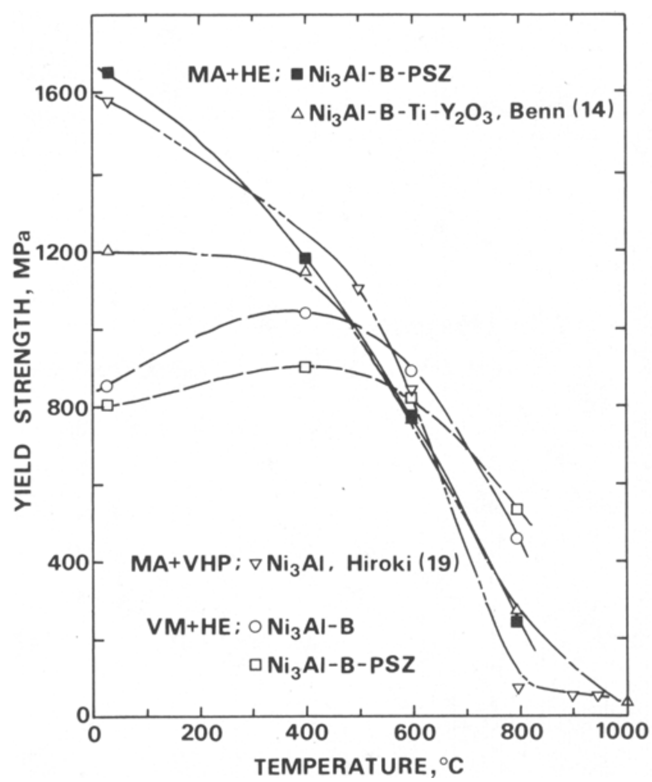

Fig. 9 Yield strength of dispersion-strengthened and hot-extruded experimental Ni_3Al-B alloys as a function of temperature. MA, mechanical alloying; VM, V-cone mixing; HE, hot extrusion; VHP, vacuum hot pressing

ing mechanical alloying. Above 800 °C, the tensile ductility improved significantly, presumably aided by boundary sliding of the fine grains.

4. Discussion

Because there is a chance of amorphization during milling, it is important to evaluate the optimum time for mechanical alloying. According to Benjamin (Ref 17), the rate of energy input during mechanical milling is constant, but that for the deforming particles is proportional to the hardness of the particles. Therefore:

$$\frac{dE}{dt} = K_1$$
$$\frac{dE}{d\varepsilon} = K_2 H_v \qquad \text{(Eq 1)}$$

where E is energy, K_1 and K_2 are constants, H_v is the Vickers microhardness, t is the milling time, and ε is the true strain. From the two equations above, the strain ε can be obtained as a function of time. The time dependence of H_v was obtained from the experimental result, as shown in Fig. 4, as follows:

$$H_v = 230 + 0.937t \qquad \text{(Eq 2)}$$

Therefore the time dependence of ε is:

$$e = 3.34 \ln (1 + 0.0041t) \text{ for } (10 \text{ min} < t < 600 \text{ min}) \qquad \text{(Eq 3)}$$

The integration constants were obtained from the experimentally observed lamellar thickness of 4.75 and 1.25 µm for $t = 0$ and $t = 120$ min, respectively. Figure 11 shows that the calculated lamellar thickness as a function of time agrees well with the experimental values. The thickness rapidly decreased with time up to 10 h, then reached a steady state at 16 h, which substantiates the conclusion obtained from the x-ray diffraction result.

In a previous work (Ref 20), the present authors suggested a Hall-Petch relationship for the extruded alloy containing PSZ as follows:

$$s_y = \sigma_0 + k_y d^{-0.85 \pm 0\ 05} \qquad \text{(Eq 4)}$$

where the units of σ and d are MPa and µm, respectively, and the values of the constants σ_0 and k_y are about 420 MPa and 2000 MPa · µm$^{0.85}$, respectively. This relationship also accounted for the behavior of the present mechanically alloyed and hot-extruded alloy. V-cone-mixed and hot-extruded alloys, however, showed a lower yield strength than the prediction because of the heterogeneous distribution of PSZ.

5. Conclusion

The present work showed that fine PSZ is a potential candidate material for dispersion hardening of intermetallic compound based on Ni_3Al-B. A processing route that consisted of mechanical alloying and hot extrusion of elemental powder mixture was proposed. Aided by fine dispersoids, the mechanically alloyed Ni_3Al-B from elemental powder mixture containing PSZ showed a remarkably high yield strength in

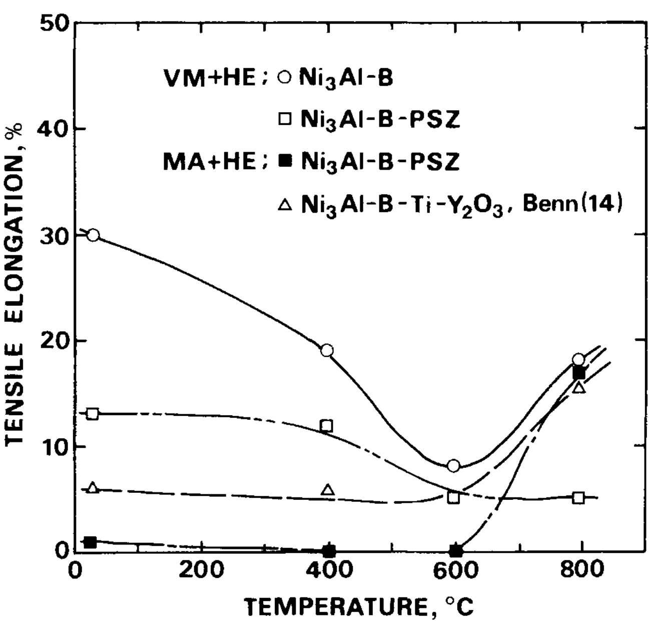

Fig. 10 Tensile elongation of dispersion-strengthened and hot-extruded experimental Ni_3Al-B alloys as a function of temperature. MA, mechanical alloying; VM, V-cone mixing; HE, hot extrusion

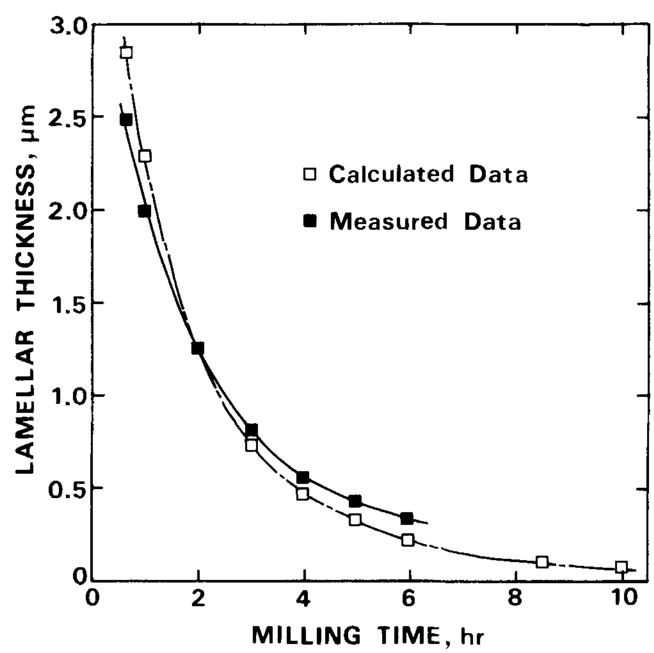

Fig. 11 Variation of the lamellar thickness as a function of time of Ni_3Al particles made by mechanical alloying of elemental powders

hot-extruded condition, although this was accompanied by a reduction in tensile ductility.

Acknowledgment

This work was supported by the Korea Science and Engineering Foundation through the Center for Advanced Aerospace Materials, POSTECH.

References

1. N.S. Stoloff, Physical Metallurgy of Ni_3Al and Its Alloys, *Int. Mater. Rev.*, Vol 34 (No. 4), 1987, p 153-183
2. V. Paidar, D.P. Pope, and V. Vitek, A Theory of the Anomalous Yield Behavior in $L1_2$ Ordered Alloys, *Acta Metall.*, Vol 32 (No. 3), 1984, p 435-448
3. K. Aoki and O. Izumi, Improvement in Room Temperature Ductility of the $L1_2$ Type Intermetallic Compound Ni_3Al by Boron Addition, *J. Jpn. Inst. Met.*, Vol 43 (No. 12), 1979, p 1190-1196
4. C.T. Liu and C.L. White, Design of Ductile Polycrystalline Ni_3Al Alloys, *High Temperature Ordered Intermetallic Alloys*, C.C. Koch, C.T. Liu, and N.S. Stoloff, Ed., Mat. Res. Soc. Symp. Proc., Vol 39, Materials Research Society, 1985, p 365-380
5. A. Bose, B.H. Rabin, and R.M. German, Reactive Sintering Nickel-Aluminide to Near Full Density, *Powder Metall. Int.*, Vol 20 (No. 3), 1988, p 25-30
6. P.S. Khadkikar, K. Vedula, and B.S. Schbel, The Role of Boron in Ductilizing Ni_3Al, *Metall. Trans. A*, Vol 18A (No. 3), 1987, p 425-428
7. C.C. Koch, Dispersoids in Intermetallic Alloys, *High Temperature Ordered Intermetallic Alloys II*, N.S. Stoloff, C.C. Koch, C.T. Liu, and O. Izumi, Ed., Mat. Res. Soc. Symp. Proc., Vol 81, Materials Research Society, 1987, p 369-380
8. C.G. Mckamey and C.A. Carmichael, Microstructure and Mechanical Properties of Ni_3Al-Based Alloys Reinforced with Particulates, *High Temperature Ordered Intermetallic Alloys IV*, L.A. Johnson, D.P. Pope, and J.O. Stiegler, Ed., Mat. Res. Soc. Symp. Proc., Vol 213, Materials Research Society, 1991, p 1051-1056
9. G.M. Camus, D.J. Duquette, and N.S. Stoloff, Effect of an Oxide Dispersion on the Hydrogen Embrittlement of a Ni_3Al Base Alloy, *J. Mater. Res.*, Vol 5 (No. 5), 1990, p 950-954
10. E.H. Yoon and S.K. Hwang, Mechanical Properties of Boron-Doped Ni_3Al Ordered Intermetallic Compounds by Powder Metallurgical Process, *J. Korean Inst. Met.*, Vol 28 (No. 10), 1990, p 887-894
11. E.H. Yoon, S.K. Hwang, Y.J. Kim, and H.S. Chung, Reactive Sintering and Hot Extrusion of PM Ni_3Al-B-ZrO_2 Alloys, *Intermetallic Compounds*, Proc. JIMIS-6, O. Izumi, Ed., Japan Institute of Metals, 1991, p 935-939
12. E.H. Yoon and S.K. Hwang, Mechanical Properties of Dispersion Strengthened Ni_3Al-B Intermetallic Compound, *J. Korean Inst. Met.*, Vol 31 (No. 7), 1993, p 897-905
13. J.S.C. Wang, S.G. Donnelly, P. Godavarti, and C.C. Koch, Microstructures and Mechanical Behavior of Mechanically Alloyed Nickel Aluminide, *Int. J. Powder Metall.*, Vol 24 (No. 4), 1988, p 315-325
14. R.C. Benn, P.K. Michandani, and A.S. Watwe, Physical Metallurgy of High Temperature Intermetallic-Based Alloys by Mechanical Alloying, *Solid State Powder Processing*, A.H. Claner and J.J. deBarbadillo, Ed., The Minerals, Metals & Materials Society, 1990, p 157-171
15. J.S.C. Wang and C.C. Koch, Amorphization and Disordering of the Ni_3Al Ordered Intermetallic by Mechanical Milling, *J. Mater. Res.*, Vol 5 (No. 3), 1990, p 498-510
16. C.C. Koch, Structural Development during Powder Milling, *Solid State Powder Processing*, A.H. Claner and J.J. deBarbadillo, Ed., The Minerals, Metals & Materials Society, 1990, p 35-53
17. J.S. Benjamin and T.E. Volin, The Mechanism of Mechanical Alloying, *Metall. Trans.*, Vol 5 (No. 8), 1974, p 1929-1934
18. B.D. Cullity, *Elements of X-ray Diffraction*, 2nd ed., Addison-Wesley, 1978, p 363-367
19. H. Esaki and M. Tokizane, High Temperature Deformation Behavior of the Ni_3Al Compacts Produced by Hot Pressing of Mechanically Alloyed Powder, *J. Jpn. Inst. Met.*, Vol 55 (No. 4), 1991, p 452-458
20. E.H. Yoon, "Ni_3Al-Based Intermetallic Compound Consolidated by Elemental Powder Process," Ph.D. thesis, Inha University, Inchon, Korea, 1993, p 117-137